Available online at www.sciencedirect.com

ScienceDirect

IFAC Papers Online CONFERENCE PAPER ARCHIVE

IFAC PapersOnLine 52-15 (2019) 579–584

Commutation Angle Iterative Learning Control: Enhancing Piezo-Stepper Actuator Waveforms

Nard Strijbosch * **Paul Tacx** * **Edwin Verschueren** ** **Tom Oomen** *

* *Eindhoven University of Technology, Department of Mechanical engineering, P.O. Box 513, 5600 MB Eindhoven (e-mail: n.w.a.strijbosch@tue.nl, p.j.m.m.tacx@student.tue.nl, t.a.e.oomen@tue.nl)*

** *Thermo Fisher Scientific, (e-mail: edwin.verschueren@thermofisher.com)*

Abstract: Piezo-stepper actuators consist of piezo elements that are able to displace a mover over an infinite stroke through walking while maintaining the high accuracy and high stiffness properties of the piezo elements. The aim of this paper is to mitigate repetitive disturbances, that are introduced by the walking behaviour, to improve the performance of piezo-stepper actuators. The key challenge is to address repeating disturbances in the position domain, which may be varying in the time domain. A new position-domain iterative learning control procedure is presented that computes a signal in the commutation angle domain that mitigates the repetitive disturbances. The results from this procedure are exploited to determine an optimal waveform for the working range of the actuator. A significant improvement in performance is achieved after applying this waveform to a piezo-stepper actuator.

Keywords: Learning Control, Actuating Signal, Piezo Actuators

1. INTRODUCTION

Piezo actuators are attractive in high precision motion systems, even for long stroke actuation due to "walking". Piezo actuators have high accuracy and high stiffness properties, however, they often have a limited stroke (Moheimani and Fleming, 2006; Uchino and Giniewicz, 2003). Piezo-stepper actuators consist of multiple piezo-elements (legs) that propel a mover by performing motions similar to walking. This allows the mover to have an infinite stroke while maintaining the stiffness properties of the individual piezo actuators, see e.g., Shamoto and Moriwaki (1997); Salisbury et al. (2007); Egashira et al. (2001).

The walking behaviour is achieved through the design of appropriate waveforms, which define the input to the individual piezo elements as a function of the commutation angle α, see e.g., Kusakawa et al. (2004). A full step of the piezo-stepper actuator is defined on the interval $\alpha \in [0, 2\pi)$ and extends periodically. The control input to the piezo-stepper actuator is the drive frequency f_α which by integration gives the commutation angle α, see e.g., Merry et al. (2011). This α generates, through the waveforms, an input signal for the individual piezo elements, which propel the mover. Piezo-stepper actuators are performing various tasks, i.e., the mover should be able to move with various velocities. Hence, an appropriate waveform achieves high performance for the complete working range.

Different type of waveforms exists, see for instance Kusakawa et al. (2004) for triangular, rectangular or sinusoidal waveforms. Selecting a waveform has a significant effect on the performance that can be achieved by a piezo-stepper actuator. Several algorithms are defined in literature to optimize the waveforms for specific objectives. In Jiang et al. (2000) a procedure is outlined to obtain the highest possible speed with a piezo-stepper actuator. In Merry et al. (2011) model-based and data-based optimization algorithms are introduced that minimize the velocity error when applying a constant drive frequency. Therefore the methods introduced in (Jiang et al., 2000; Merry et al., 2011) will result in an optimal waveform for a specific velocity, the high performance for other velocities in the working range is not guaranteed.

Experiments with a piezo-stepper actuator reveal that disturbances are present in piezo-stepper actuators, see e.g., Merry et al. (2011). These errors can be directly related to the walking behaviour of a piezo-stepper actuator, i.e. the commutation angle. Several control algorithms, such as iterative learning control (ILC), focus on compensating for the reproducible part of the error to achieve a significant increase in performance, see e.g., Bristow et al. (2006). These temporal ILC techniques techniques can be applied to mitigate the reproducible part of the error for a specific task and cannot be applied to obtain performance improvements for varying tasks.

Several ILC approaches outside the temporal domain have been developed, see e.g., Hoelzle and Barton (2016); Kong et al. (2015). In Hoelzle and Barton (2016) temporal dynamics are ignored to obtain a static system in the time domain, which is exploited in a 2D spatial ILC approach.

⋆ This work is part of the research programme VIDI with project number 15698, which is (partly) financed by the Netherlands Organisation for Scientific Research (NWO).

10.1016/j.ifacol.2019.11.738

This method is developed for additive manufacturing systems where the output of the system can be measured at a fixed number of discrete points in the spatial domain. This is not the case for piezo steppers as the value of the commutation angle can be any value in a continuous interval. Moreover, in Kong et al. (2015) an ILC approach is developed that indexes previous iterations of a bipedal walking robot by a phase variable. This method assumes that in the limit stable periodic walking is obtained with an unknown period time. For piezo-stepper actuators, this assumption is not valid as the input drive frequency could lead to various velocities, i.e., varying period times.

Although several waveform optimization techniques are available, there is no method that exploits the repeatability of the error. Consequently, for each of these methods, an error will remain that can be compensated through learning. The aim of this paper is to develop an ILC algorithm capable of compensating the highly reproducible errors in the commutation angle domain. The resulting input signal for the piezo-elements is given as a function of the commutation angle, α. Moreover, it is outlined how this input signal can be translated into a waveform. This waveform mitigates the reproducible part of the error in the commutation angle domain, therefore it is optimal for the complete working range of the piezo-stepper actuator.

The main contribution of this paper is a waveform optimization procedure that exploits ideas from ILC. This is achieved through the following sub-contributions.

- C1 In Section 2, the problem of finding an optimal waveform for a piezo-stepper actuator is elaborated.
- C2 In Section 3, it is revealed that disturbances observed from piezo-stepper actuators are highly reproducible in the commutation angle domain.
- C3 In Section 4, a commutation angle domain iterative learning control based algorithm is developed that mitigates the reproducible part of these disturbances.
- C4 In Section 5, a procedure is outlined that translates the obtained input signals into a waveform.
- C5 In Section 6, the implementation aspects of the ILC algorithm are provided. Finally, experimental results show a significant improvement.

2. PROBLEM FORMULATION

2.1 Piezo-stepper actuator

Piezo-stepper actuators consist out of longitudinal and shear piezo elements that are able to change the position of a mover. A possible configuration of the piezo elements is depicted in Fig. 1, see also Shamoto and Moriwaki (1997); Salisbury et al. (2007); Naikwad et al. (2016) for alternative configurations. The piezo elements are ordered in 2 groups. Each group consist out of three shear elements (S1 and S2) and a longitudinal piezo element (C1 and C2) referred to as clamp. When the longitudinal piezo elements are extended, the corresponding shear elements are in contact with the mover. If a voltage is applied to these shear elements in this position, the mover follows the displacement of the shear elements. The walking behaviour is achieved by alternating the two piezo groups leads to a possibly infinite stroke of the mover.

2.2 Actuation of piezo elements

To achieve the walking behaviour a set of waveforms, define the relation between the inputs of the individual

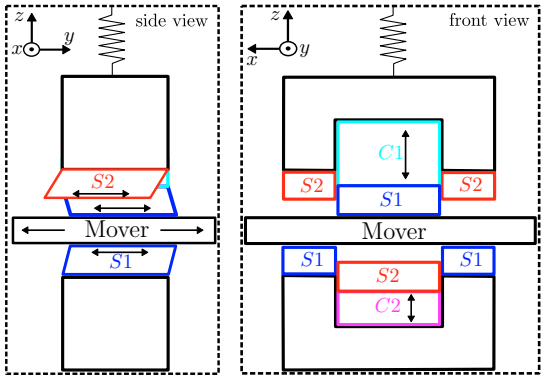

Fig. 1. Side view (left) and front view (right) of piezo-stepper actuator. The different piezo elements are: clamping piezo of group 1 (—); clamping piezo of group 2 (—); shear piezo of group 1 (—); shear piezo of group 2 (—);

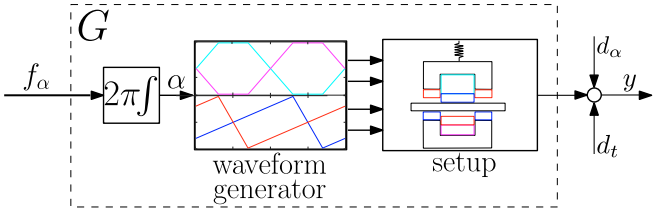

Fig. 2. Open-loop implementation of waveforms to actuate the piezo walk actuator. From the input f_α (drive frequency) to the output y (Mover position)

piezo elements. The waveforms are mappings from the commutation angle $\alpha \in \mathbb{R}$ to the input voltage $V \in \mathbb{R}$ of the piezo elements. The waveforms are defined on the interval $\alpha \in [0, 2\pi)$ and extend periodically on $\alpha \in \mathbb{R}$. A full step cycle from $\alpha = 0$ to $\alpha = 2\pi$ corresponds to a step of the first piezo group followed by a step from the second piezo group. The waveforms for the longitudinal piezo elements of the first and second group are denoted by $c_1(\alpha)$ and $c_2(\alpha)$, respectively. The waveforms for the shear elements of the first and second group are denoted by $s_1(\alpha)$ and $s_2(\alpha)$, respectively. The relation between the input voltage $s_i(\alpha(t))$ and the displacement of the corresponding shear piezo element, $y_i(t)$, is static, i.e.,

$$y_i(t) = cs_i(\alpha(t)) \tag{1}$$

with $c \in \mathbb{R}_{>0}$ a constant dependent on the piezo electric material (Moheimani and Fleming, 2006; Uchino and Giniewicz, 2003).

The waveforms are implemented as in Fig. 2, where the output y is the position of the mover and the input f_α is the drive frequency, defined as the number of step cycles the piezo-stepper actuator performs each time unit. The commutation angle α is defined as

$$\alpha(t) = 2\pi \int_0^t f_\alpha(\tau)\, \mathrm{d}\tau. \tag{2}$$

The commutation angle α for a given drive frequency signal f_α is presented in Fig. 3.

The waveforms are designed to obtain a linear relation between the commutation angle $\alpha(t)$ and the expected mover displacement $y_e(t)$, i.e.,

$$y_e(t) = \kappa\alpha(t) = \kappa 2\pi \int_0^t f_\alpha(\tau)\, \mathrm{d}\tau, \tag{3}$$

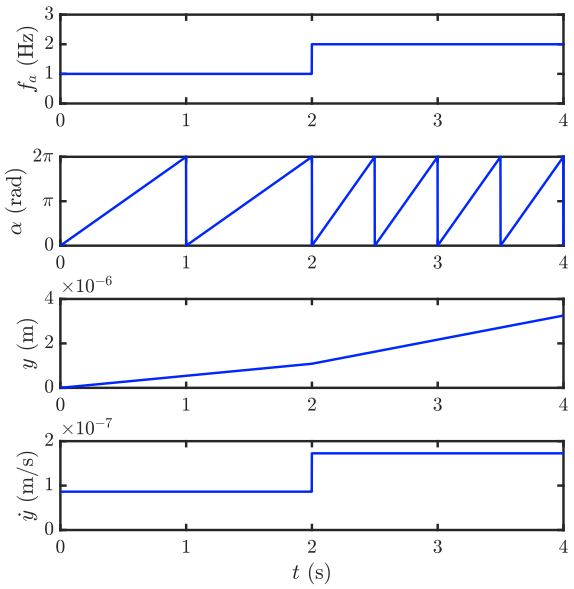

Fig. 3. For a given input signal f_α the corresponding commutation angle α, position y and velocity $\dot{y}$.

with constant $\kappa \in \mathbb{R}_{>0}$ dependent on the piezo electric material. The expected position y_e and its time derivative $\dot{y}_e$ for a given driven frequency signal $f_\alpha(t)$ and κ are presented in Fig. 3. Notice that $\dot{y}_e(t) = \kappa f_\alpha(t)$.

Note that hysteresis and creep effects are neglected in (1). If hysteresis effects are significant, this can be effectively compensated for by exploiting, for instance, charge control to obtain the linear relation to the applied charge (Comstock, 1981; Newcomb and Flinn, 1982; Moheimani and Fleming, 2006). Moreover, creep effects can be neglected as the time constant of creep is in the order of a few minutes (Fleming and Leang, 2014), which is large compared to the lenght of a step which is in the order of seconds.

2.3 Disturbances

During open-loop experiments, the expected relation (3) is not obtained, as will be experimentally shown. The disturbances that cause this error could have different sources. One of these could be an incorrect alignment of the piezo elements. If for instance, a longitudinal piezo element is not exactly perpendicular to the mover a force is present in the y direction. Besides this, contact dynamics can influence the position when the shear elements come in contact with the mover, this can cause a hammering effect (Van Brussel et al., 2003). Moreover, differences in the properties of the piezo elements can cause differences in the velocity of each piezo element.

The mentioned disturbances can be modelled by two lumped disturbances $d_\alpha(\alpha)$ and $d_t(t)$. The disturbance d_α captures all disturbances that can directly be related to the commutation angle, all other disturbances are captured by d_t. Throughout this paper, it is assumed that the following hypothesis is valid,

Hypothesis 1. The disturbance d_α is dominant compared to the disturbance d_t, i.e. $d_\alpha >> d_t$.

Hypothesis 1 allows to write the position of the mover, during clamping experiments, as

$$y(t) = cu(t) + d_\alpha(\alpha(t)) \tag{4}$$

with $u(t)$ the input voltage to the shear piezo elements. During clamping experiments the input to the shear piezo elements $u(t) = 0$. However, from (4) it is obvious that there exist an input as function of α, i.e, $u(\alpha(t))$ that compensates for this disturbance.

The aim of this paper is to exploit ideas from iterative learning control to determine a new waveform that compensates for the disturbance d_α. Common used ILC algorithms are designed to compensate for reproducible disturbances in the temporal domain (Bristow et al., 2006). Due to the nature of the disturbance d_α, in this paper, the problem of designing an ILC algorithm to compensate for disturbances in the α-domain is addressed. Moreover, the problem of translating this control input into a waveform is addressed.

3. DISTURBANCE ANALYSIS

In this section Hypothesis 1 is tested through experiments. To identify the disturbances d_α and d_t initial experiments on a piezo-stepper actuator are performed. During these experiments a piezo-stepper actuator with a configuration as in Fig. 1 is used. Two type of experiments are performed, defined as follows.

Definition 2. (Open-loop Walking Experiment). A signal $f_\alpha(t)$ is applied to the open-loop control configuration as depicted in Fig. 2 with the waveforms from Fig. 5. The displacement of the mover, $y(t)$, is measured. The expected relation between the input signal $f_\alpha(t)$ and the position $y(t)$ is given by (3) for a certain $\kappa \in \mathbb{R}_{>0}$.

Definition 3. (Open-loop Clamping Experiment). A signal $f_\alpha(t)$ is applied to the open-loop control configuration as depicted in Fig. 2 with the waveforms from Fig. 5. However, only the clamping piezo elements will be active, i.e, $s_1(\alpha) = s_2(\alpha) = 0$. The displacement of the mover, $y(t)$, is measured. The shear piezo elements are stationary, hence the expected position of the mover $y_e(t) = 0$.

It is not possible to analyse the error $e(t) = y_e(t) - y(t)$ from an open-loop walking experiment as the exact value of the constant κ is unknown. In a clamping experiment the error $e(t) = y_e(t) - y(t) = -y(t)$ can be evaluated. Hence, these experiments are used to analyse the disturbances d_α and d_t. However, open-loop clamping experiments will be performed to analyse the walking behaviour of the piezo-stepper actuator in Section 6.

To identify which part of the error is a function of the commutation angle the position of several open-loop clamping experiments with various drive frequencies $f_\alpha(t)$ are presented in the temporal domain and α-domain in Fig. 4. When evaluating the error in the commutation angle domain it is observed that the errors are highly reproducible. There is no correlation between the experiments when evaluating this error in the temporal domain. From this observation, it is concluded that Hypothesis 1 is valid.

4. α-DOMAIN ITERATIVE LEARNING CONTROL

In this section, the α-domain ILC framework is developed. This procedure consists out of performing consecutive clamping experiments referred to as trials to find an input signal for the shear piezo elements that compensate the reproducible part of the error. A signal x during the j-th trial is denoted by x_j.

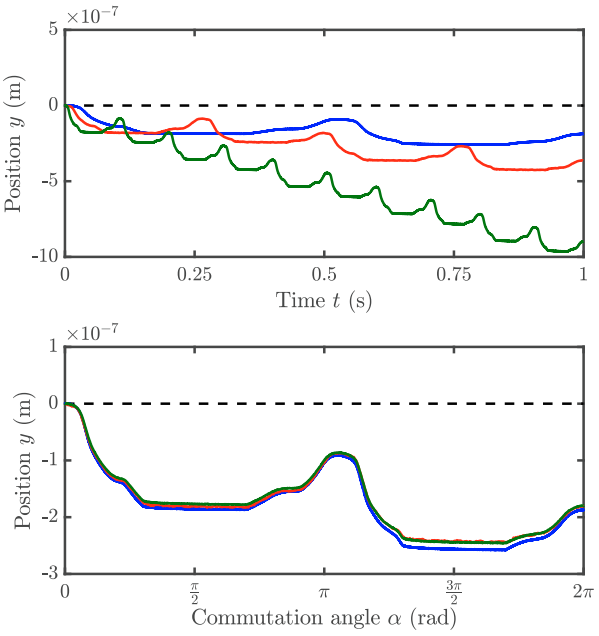

Fig. 4. Measured position y and expected position $y_e = 0$ (- -) during clamping experiments for various step frequencies. Experiments are performed with constant drive frequency $f_\alpha = 1$ Hz (—), $f_\alpha = 2$ Hz (—), and $f_\alpha = 5$ Hz (—).

4.1 Assumptions

First, a set of assumptions is imposed parallel to the assumptions imposed in temporal ILC.

In a standard temporal ILC setting the experiments are all of the same length, i.e., $t \in [0, T]$. Moreover, the systems start each experiment with identical initial conditions. If these conditions are satisfied experiments with identical inputs $u_j(t)$, lead to identical errors $e_j(t)$. Which is the key assumption in temporal ILC. Due to this, the error from trial j can be exploited to determine an input u_{j+1} that compensates for this observed error in the next trial.

Parallel to these assumptions, the following assumptions are imposed for α-domain ILC.

Assumption 4. The initial condition condition $y_j(0)$ is identical for each trial j.

Assumption 5. Each trial is of constant length in the α-domain, i.e., $\alpha_j \in [0, 2\pi]$.

Assumption 6. For each trial j there exists a mapping $F_j : [0, T_j] \mapsto [0, 2\pi]$ that uniquely maps the time interval $t \in [0, T_j]$ of the trial to the commutation angle interval $\alpha \in [0, 2\pi]$.

Assumption 4 can easily be satisfied by compensating for the initial offset of the mover in the measurement signal. Assumption 5 is satisfied by chosing a measurement time such that $\alpha(T_j) = 2\pi$. Notice, that this allows for trials with varying length in the temporal domain. Assumption 6 is satisfied if either $f_\alpha(t) > 0$ or $f_\alpha(t) < 0$ for $t \in [0, T_j]$, i.e., α is continuously increasing or decreasing.

Due to the unique mapping F_j the inverse mapping $F_j^{-1} : [0, 2\pi] \mapsto [0, T_j]$ exists. This allows to map a given signal in the temporal domain as a signal in the α-domain, i.e.

$$\bar{y}_j(\alpha) = y_j(F_j^{-1}(\alpha)), \text{ and } \bar{u}_j(\alpha) = u_j(F_j^{-1}(\alpha)). \quad (5)$$

4.2 α-domain ILC algorithm

Exploiting (5) the system (4) can be fully described in the α-domain as

$$\bar{y}_j(\alpha) = c\bar{u}_j(\alpha) + d(\alpha),\ \alpha \in [0, 2\pi]. \quad (6)$$

with $\bar{u}_j(\alpha)$ the input signal applied to both shear groups. Moreover, the error, $\bar{e}_j(\alpha)$ is defined as

$$\bar{e}_j(\alpha) = \bar{y}_e(\alpha) - \bar{y}_j(\alpha) = -\bar{y}_j(\alpha). \quad (7)$$

Based on a P-type ILC update law in temporal domain, see e.g., Bristow et al. (2006), the following α-domain ILC update law is introduced for (6):

$$\bar{u}_{j+1}(\alpha) = \bar{u}_j(\alpha) + \gamma\bar{e}_j(\alpha), \quad (8)$$

with $\gamma \in \mathbb{R}_{>0}$. This reduces the ILC problem to selecting a $\gamma \in \mathbb{R}_{>0}$ such that the sequence of errors $\{\|e_j\|\}_{j\in\mathbb{N}}$ converges to a unique e_∞.

Remark 7. Notice, that standard temporal P-type ILC is recovered from (8) and (5) when identical experiments with constant drive frequency are performed, Bristow et al. (2006). The α-domain ILC approach allows for trial varying drive frequencies. Therefore an input signal $u_\infty(\alpha)$ can be found that is optimal for a range of drive frequencies, where general P-type ILC can only guarantee that the input $u_\infty(\alpha)$ is optimal for a single drive frequency.

4.3 Convergence Analysis

Following a similar convergence analysis as for temporal ILC the following result is obtained:

Theorem 8. (Convergence α-domain ILC). Consider system (6) and update law (8). Then the sequence of errors $\{\|e_j\|\}_{j\in\mathbb{N}}$ converges to a unique e_∞ if and only if $\gamma \leq \frac{1}{c}$. Moreover, the convergence rate is given by $|1 - c\gamma|$

5. WAVEFORM OPTIMIZATION

In this section, a procedure is outlined that exploits the results obtained from the α-domain ILC procedure in previous section to obtain a waveform. To achieve this, first the basic design principles for waveforms are elaborated.

5.1 Design principles waveform

The set of waveforms currently applied to the piezo-stepper actuator are triangular waveforms as depicted in Fig. 5. For each of the waveforms s_1 and s_2 two intervals can be distinguished. In the first interval, the corresponding clamping piezo element is (partly) extended. In the second interval, the corresponding clamping piezo element is fully retracted, indicated by A and B in Fig. 5.

In the interval where a clamping piezo element is (partly) extended, the corresponding group of shear piezo elements is (possibly) in contact with the mover. In the intervals where possibly both shear piezo groups can be in contact with the mover, the waveforms $s_1(\alpha)$ and $s_2(\alpha)$ satisfy

$$\frac{\partial s_1(\alpha)}{\partial \alpha} = \frac{\partial s_2(\alpha)}{\partial \alpha}. \quad (9)$$

This relation ensures that both shear piezo groups move with the same velocity. Due to this, the velocity of the mover is equivalent to the velocity of the shear piezo elements, and no internal forces act on the mover.

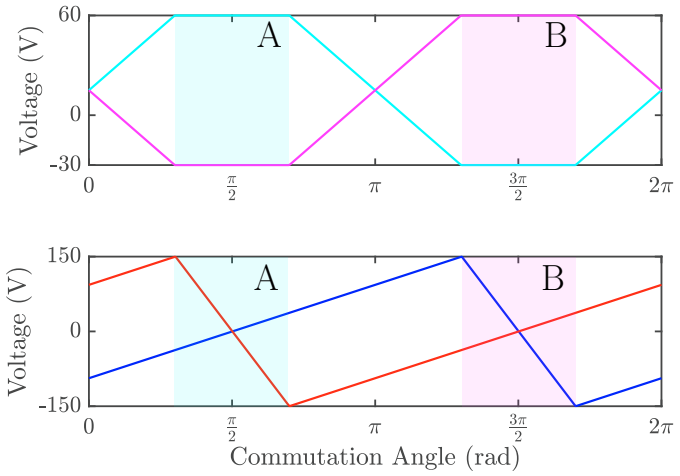

Fig. 5. Top: waveforms applied to clamping piezo elements, $c_1(\alpha)$ (—), $c_2(\alpha)$ (—).
Bottom: waveforms applied to shear piezo elements, $s_1(\alpha)$ (—), $s_2(\alpha)$ (—).
The area in cyan ( ) indicates the interval where the clamp piezo elements of group 1 is fully extended and the shears of group 2 are not in contact with the mover. The area in magenta ( ) indicates the interval where the clamp piezo elements of group 2 is fully extended and the shears of group 1 are not in contact with the mover.

The intervals where the clamping piezo elements are fully retracted are exploited to reset the shear piezo elements to their most outer position. This ensures that the waveforms s_1 and s_2 can be periodically extended, i.e. the following is satisfied

$$s_i(0) = s_i(2\pi),\ i \in \{1, 2\} \tag{10}$$

The retracting can be observed in Fig. 5, in the intervals A and B. In Interval A the shears of group 2 are not in contact with the mover as its corresponding clamp piezo is fully retracted. In this interval, the waveform is defined to reset the shear piezo elements to their most outer position. In Interval B the shears of group 1 are not in contact, hence the waveforms for the shear piezo elements of this group are defined to reset the shear piezo elements to their most outer position.

5.2 Determine waveform from α-domain ILC results

The input signal $u_\infty(\alpha)$ that is obtained from the α-domain ILC procedure outlined in the previous section can not directly be applied as a waveform, as it cannot be periodically extended if $u_\infty(0) \neq u_\infty(2\pi)$. Hence, the input signal $u_\infty(\alpha)$ should be altered to obtain two waveforms, $z_1(\alpha)$ and $z_2(\alpha)$, which should be applied to the first shear group and second shear group, respectively. To maintain identical performance, the time where a shear group is not in contact with the mover is exploited to reset the shear elements such that $u(0) = u(2\pi)$. When a shear group is possibly in contact the following should be satisfied

$$\frac{\partial u_\infty}{\partial \alpha} = \frac{\partial z_1(\alpha)}{\partial \alpha} \quad = \frac{\partial z_2(\alpha)}{\partial \alpha}. \tag{11}$$

Similar to condition 9 this condition ensures that the velocity of the shears that are in contact have identical velocity. This velocity is dictated by the velocity of the function u_∞. The procedure to determine $z_1(\alpha)$ and $z_2(\alpha)$ from a given signal $u(\alpha)$ is depicted in Fig. 7.

Applying the waveforms z_1 and z_2 will lead to identical performance as applying the input signal u_∞ during an open-loop clamping experiment. Moreover, a significant performance improvement can be achieved during open-loop walking experiments if the waveforms z_1 and z_2 are added to the waveforms s_1 and s_2, i.e.,

$$s_1'(\alpha) = s_1(\alpha) + z_1(\alpha), \quad s_2'(\alpha) = s_2(\alpha) + z_2(\alpha). \tag{12}$$

When these waveforms are applied all disturbances caused by clamping of the piezo elements are mitigated during open-loop walking experiments, hence a significant performance increase is achieved.

6. EXPERIMENTAL RESULTS

In this section, the α-domain ILC approach is applied to a piezo walking actuator. During the experiments, a configuration of piezo elements as given in Fig. 1 is used. The waveforms for the actuator are given in Fig. 5. Before applying the α-domain ILC approach to determine an input signal $u(\alpha)$ for the shear piezo elements, some implementation aspects are discussed. Next, these results are used to obtain a waveform to increase the performance of the piezo-stepper actuator during an open-loop walking experiment.

6.1 Implementation aspects

As the piezo-stepper actuator is implemented using a digital controller the signals obtained during experiments are sampled with a sample frequency of 10 kHz. Hence, discrete-time signals are available instead of continuous-time signals. Consequently, only discrete data points are available in the α-domain. This discrete data points are possibly non-equidistant in the α-domain. Moreover, the number of discrete-time data points possibly vary each iteration. To obtain continuous-time signals in the α-domain a parametrization of the signals is exploited.

The waveforms are typically defined by a set of points $\bar{u}(\alpha_k)$ where $\alpha_k := \frac{2\pi k}{N-1}, k \in [0, N]$ with N the number of points, such that

$$u(\alpha) = \bar{u}(\alpha_k) + \frac{\bar{u}(\alpha_{k+1}) - \bar{u}(\alpha)}{\alpha_{k+1} - \alpha_k}, \text{for } \alpha \in [\alpha_k, \alpha_{k+1}]. \tag{13}$$

Due, to this parametrization of the waveforms it is natural to map the discrete-time signals from the experiments to the discrete-data points α_k by means of linear interpolation. Note that other parametrizations of the signals in the α-domain can be considered.

6.2 α-domain ILC applied on experimental setup

In Fig. 6 the convergence of the sequence of errors $\{e_j\}_{j\in\mathbb{N}}$ during clamping experiments with varying drive frequencies is presented. This result is obtained by applying α-domain ILC update law (8) and the parametrization of the waveform (13). A significant improvement of the error signal can be observed.

6.3 Applying optimized waveform

The input signal applied to the shears during trial 17, $u_{17}(\alpha)$ is presented in Fig. 7. It can be observed that the input signal $u_{17}(0) \neq u_{17}(2\pi)$, hence the procedure as discussed in Section 5 is used to determine the waveforms $z_1(\alpha)$ and $z_2(\alpha)$, see Fig. 7.

When implementing the waveforms $s_1'(\alpha)$ and $s_2'(\alpha)$ as defined by (12) in a open-loop walking experiment a significant increase in performance is observed, see Fig. 8.

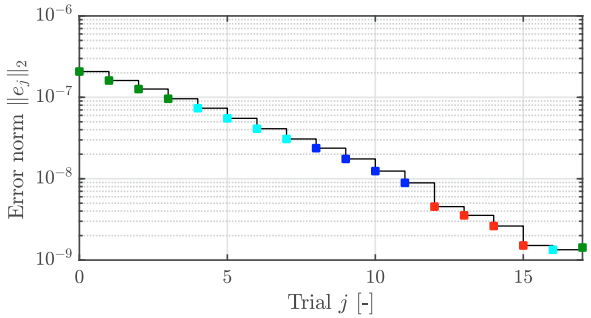

Fig. 6. Error norm $\|\bar{e}_j\|_2$ for each trial. Experiments are performed with constant drive frequency: $f_\alpha = 1$ Hz (■); $f_\alpha = 2$ Hz (■); $f_\alpha = 5$ Hz (■); $f_\alpha = 10$ Hz (■).

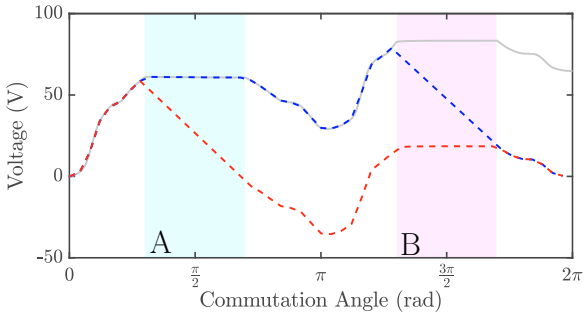

Fig. 7. Feedforward signal obtain at trial 17, $u_{17}(\alpha)$ (—). Corresponding waveforms for the first group, $z_1(\alpha)$, (- -) and second group, $z_2(\alpha)$, (- -).

7. CONCLUSION

An ILC framework is developed for systems that are subject to disturbances which are reproducible in the commutation angle domain, results obtained from this procedure enables enhanced walking behaviour for piezo-stepper actuators, which is illustrated by promising experimental results. First, it is revealed that disturbances in the error observed from piezo-stepper actuators are highly reproducible with respect to the commutation angle. Based on this observation an ILC algorithm is developed that mitigates the reproducible part of the observed error. The input signal obtained from the ILC algorithm is exploited to determine a new waveform to increase the performance of the piezo-stepper. Finally, experimental results show a significant performance increase when exploiting the developed optimization procedure.

ACKNOWLEDGEMENT

The authors wish to thank Leontine Aarnoudse for performing revised and expanded experiments.

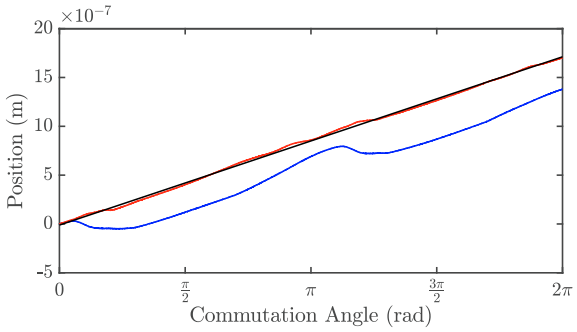

Fig. 8. Mover position during walking experiment: ideal (—); original waveforms (—); optimized waveforms (—).

REFERENCES

Bristow, D.A., Tharayil, M., and Alleyne, A.G. (2006). A survey of iterative learning control. *IEEE Control Systems Magazine*, 26(3), 96–114.

Comstock, R.H. (1981). Charge control of piezoelectric actuators to reduce hysteresis effects. US Patent 4,263,527.

Egashira, Y., Kosaka, K., Takada, S., Iwabuchi, T., Baba, T., Moriyama, S., Harada, T., Nagamoto, K., Nakada, A., Kubota, H., and Ohmi, T. (2001). 0.69 nm resolution ultrasonic motor for large stroke precision stage. In *Proceedings of the 2001 1st IEEE Conf. on Nanotechnology. IEEE-NANO 2001 (Cat. No.01EX516)*, 397–402.

Fleming, A.J. and Leang, K.K. (2014). *Design, modeling and control of nanopositioning systems*. Springer.

Hoelzle, D.J. and Barton, K.L. (2016). On spatial iterative learning control via 2-d convolution: Stability analysis and computational efficiency. *IEEE Transactions on Control Systems Technology*, 24(4), 1504–1512.

Jiang, T., Ng, T., and Lam, K. (2000). Optimization of a piezoelectric ceramic actuator. *Sensors and Actuators A: Physical*, 84(1), 81 – 94.

Kong, F.H., Boudali, A.M., and Manchester, I.R. (2015). Phase-indexed ILC for control of underactuated walking robots. In *2015 IEEE Conference on Control Applications (CCA)*, 1467–1472.

Kusakawa, T., Torii, A., Doki, K., and Ueda, A. (2004). Control waveforms applied to piezo elements used in a miniature robot. In *Micro-Nanomechatronics and Human Science, 2004 and The Fourth Symposium Micro-Nanomechatronics for Information-Based Society, 2004.*, 307–312.

Merry, R.J.E., Maassen, M.G.J.M., van de Molengraft, M.J.G., van de Wouw, N., and Steinbuch, M. (2011). Modeling and waveform optimization of a nano-motion piezo stage. *IEEE/ASME Transactions on Mechatronics*, 16(4), 615–626.

Moheimani, S.R. and Fleming, A.J. (2006). *Piezoelectric transducers for vibration control and damping*. Springer Science & Business Media.

Naikwad, S., Vandervelden, R., and Hosseinnia, S.H. (2016). A novel hybrid self-sensing method for force estimation in a piezo-stepperactuator. In *Proceedings of the 4th ICCMA*, 162–167. ACM, New York, NY, USA.

Newcomb, C.V. and Flinn, I. (1982). Improving the linearity of piezoelectric ceramic actuators. *Electronics Letters*, 18(11), 442–444.

Salisbury, S.P., Waechter, D.F., Mrad, R.B., Prasad, S.E., Blacow, R.G., and Yan, B. (2007). Closed-loop control of a complementary clamp piezoworm actuator. *IEEE/ASME Trans. on Mech.*, 12(6), 590–598.

Shamoto, E. and Moriwaki, T. (1997). Development of a walking drive ultraprecision positioner. *Precision Engineering*, 20(2), 85 – 92.

Uchino, K. and Giniewicz, J. (2003). *Micromechatronics*. CRC Press.

Van Brussel, H., Reyneerts, D., Vanherck, P., Versteyhe, M., and Devos, S. (2003). A nanometre-precision, ultra-stiff plezostepper stage for ELID-grinding. *CIRP Annals-Manufacturing Technology*, 52(1), 317–322.